ILASS–Europe 2017, 28th Conference on Liquid Atomization and Spray Systems, 6-8 September 2017, Valencia, Spain
http://dx.doi.org/10.4995/ILASS2017.2017.4746

Influence of the chemical mechanism in the frame of diesel-like CFD reacting spray simulations using a presumed PDF flamelet-based combustion model

F. Payri, J. M. García-Oliver, R. Novella, E. J. Pérez-Sánchez*
CMT Motores Térmicos, Universitat Politècnica de València, Spain
*Corresponding author: edpresnc@mot.upv.es

Abstract
The ability of a computational fluid dynamics (CFD) simulation to reproduce the diesel-like reacting spray ignition process and its corresponding flame structure strongly depends on both the fidelity of the chemical mechanism for reproducing the oxidation of the fuel and also on how the turbulence-chemistry interaction (TCI) is modeled. Therefore, investigating the performance of different chemical mechanisms not only in perfect stirred reactors but directly in the diesel-like spray itself is of great interest in order to evaluate their suitability for being further applied to CFD engine simulations.
This research work focuses on applying a presumed probability density function (PDF) unsteady flamelet combustion model to the well-known spray A from the Engine Combustion Network (ECN), using three chemical mechanisms widely accepted by the scientific community as a way to figure out the influence of chemistry in the key characteristics of the combustion process in the frame of diesel-like spray simulations. Results confirm that in spite of providing all of them correct trends for ignition delays (ID) and lift-off lengths (LOL), when comparing with experimental results, the structure of the flame presents noticeable differences, especially in the low and intermediate temperatures and high equivalence ratio regions. Consequently, the selection of the chemical mechanism has an impact on the zones of influence of key species as observed in both spatial coordinates and also in the equivalence ratio-temperature maps. These differences are expected to be relevant considering the implications when coupling pollutant emissions models. The analysis of temperature and oxygen concentration parametric studies evidences how the observed differences are consistent and moderately dependent on the ambient conditions.

Keywords
Combustion modeling, Chemical mechanism, Spray A, Flamelet

Introduction

The improvement of the combustion technologies in industrial devices, such as diesel engines, in terms of efficiency and pollutant emissions, evidence that a comprehensive knowledge of the processes involved is mandatory. Between the different processes that concur in the energetic transformation, turbulent non-premixed combustion appears as one of the most relevant. Nevertheless, its modeling is a complex issue due to the different length and time scales of the turbulence, the fuel oxidation and the interaction between them [1].
These considerations point out that for a proper modeling of the turbulent non-premixed combustion two main aspects are essential. The first one is the chemical mechanism, that determines the fuel oxidation, while the second one is the turbulence-chemistry interaction (TCI).
Promoted by the need of gaining a very detailed knowledge in these issues in diesel spray conditions, the Engine Combustion Network (ECN) has proposed a set of experiments in controlled conditions that shed light for these concerns by means of experiments and numerical simulations.
More particularly, the well-known spray A models a diesel-like spray with n-dodecane as a surrogate diesel fuel. The boundary conditions encompass low temperatures and moderate EGR in correspondence with boundary conditions of interest for modern diesel engines.
On the one hand, with regard to experimental measurements, different institutions have carried out experiments with different facilities that are classified in constant-volume pre-burn (CVP) combustion vessels and constant-pressure flow (CPF) rigs [3]. With such facilities, measurements of global combustion parameters, such as ignition delay (ID) and lift-off length (LOL), together with more detailed information, such as species spatial evolution by means of planar laser-induced fluorescence (PLIF), can be captured. This valuable data permits to validate the combustion models and figure out the main aspects of the turbulent combustion.
On the other hand, with regard to the combustion modeling, it is desirable that the model reproduces the combustion structure as well as the TCI with low computational cost while managing complex chemical mechanisms for the sake of a chemically accurate evolution. These aspects are covered by flamelet models used together with tabulated chemistry and, more particularly, by the Approximated Diffusion Flamelet (ADF) approach [4]. This model, used in the present work, has been demonstrated to offer powerful capabilities and provides satisfactory results in the frame of diesel sprays and diesel engines simulations [5, 6].
Nevertheless, the fuel oxidation process, given by the chemical mechanism, arises as one of the cornerstones in the combustion numerical simulation and is one of the inputs to the problem which causes a greater uncertainty. These reasons justify the effort invested by the scientific community for properly describing the chemistry evolution that is patent in the great variety of chemical mechanisms available for a given fuel. Encouraged by this situation,

a comparison between different chemical schemes is carried out not only in homogeneous conditions, as in homogeneous reactors (HRs) calculations, but on the diesel spray itself in order to figure out the final implications of the selection of the chemical mechanism.
The aim of this work is to simulate the spray A by means of the presumed PDF ADF unsteady flamelet model with different chemical mechanisms of interest in order to clear up the implication on the choice of each of them. Experimental results were measured in CPF experimental facility available at CMT-Motores Térmicos [7, 8].
This work starts with a brief description of the model and the spray A parametric studies included. The validation is sequentially performed, first, by means of HRs and flamelet solutions and, second, by the comparison of the spray evolutions. In this case, a first analysis is given by the ID and LOL parameters, later a more detailed insight is accomplished by the species fields in spatial coordinates and equivalence ratio-temperature maps. Finally, a temporal evolution of the production of species of interest in the whole domain closes the comparison. The work ends with the main conclusions extracted from the analysis.

Methodology

Model description

Spray A has been modeled and computed in the open tool-box OpenFoam environment [9]. Cylindrical symmetry is supposed and, consequently, calculation is performed on a meridian cut, with dimensions 54 $\times$ 108 mm. The mesh is structured with constant cell size of 0.25 $\times$ 0.5 mm as in previous works [6, 10].
A RANS (Reynolds Averaged Navier-Stokes) approach is used for simulating the turbulence. More particularly, a standard $k-\varepsilon$ model with $C_{\varepsilon 1}$ =1.52 [11] is applied to calculations (the rest of constants with standard values) . The liquid phase is modeled with a DDM (discrete droplet method) based on the Kelvin-Helmholtz and Rayleigh-Taylor instabilities for describing the atomization and breakup processes in conjunction with the Ranz-Marshall model for droplet evaporation. A detailed description of the model constants used for these simulations can be found in a previous work of the authors [6].
The combustion model is based on the flamelet concept which describes the turbulent combustion as an ensemble of laminar flames, called flamelets, embedded in the turbulent flame. The flamelet equations lead to the Diffusion Flamelet (DF) model. This flame description has been successfully applied for diesel engine and gas turbines simulations [12].
The DF model solves eq. (1) for all the species (N) appearing in the chemical mechanism [1].

$$\frac{\partial Y_k}{\partial t} = \frac{\chi}{2}\frac{\partial^2 Y_k}{\partial Z^2} + \dot{\omega}_k \qquad k = 1, \ldots, N \tag{1}$$

where Y_k is the mass fraction for species k, Z is the mixture fraction, χ is the scalar dissipation rate and the chemical source term is represented by $\dot{\omega}_k$, which is obtained from the chemical ODE system.
The initial mixture fraction-temperature profile for the laminar flamelet calculations is obtained assuming an adiabatic mixing process between the air and the fuel streams, which accounts for the enthalpy exchange due to the fuel evaporation. Thus, the initial temperature for each mixture fraction decreases compared to the non-evaporative adiabatic mixing process ([13]). As the fuel is injected in liquid phase and Z only accounts for the contribution of the gas phase, Z varies between 0 and the saturation mixture fraction Z_{sat}, defined as the maximum mixture fraction for which the fuel does not condensate.
The value of χ is given by $\chi = 2D|\nabla Z|^2$, with D the molecular mass diffusion. If a steady profile is imposed, it follows the formula [1]

$$\chi(a, Z) = \frac{a}{\pi} Z_{sat}^2 \exp[-2(\mathrm{erfc}^{-1}(2Z/Z_{sat}))^2] \tag{2}$$

where a is the strain rate.
When complex mechanisms are used for diesel engine simulations, where boundary conditions vary significantly, the number of flamelets to be calculated is in the order of several hundred or thousand and solving the ODE system given by the chemical mechanism together with the PDE system given by eq. (1) is unaffordable [14]. This situation appeals for the introduction of new hypotheses that reduce the computational cost while still managing complex chemical mechanisms.
With this purpose, the ADF (Approximated Diffusion Flamelet) model was suggested several years ago in order to perform diesel engine simulations while keeping the combustion flamelet structure and using complex chemical schemes. Based on the fact that eq. (1) shows that the flamelet evolution corresponds to a homogeneous reactor (HR) when the strain rate tends to zero, the ADF model decouples the chemistry from diffusion taking the chemical source term from an equivalent homogeneous reactor. Equation for the ADF model reads

$$\frac{\partial Y_c}{\partial t} = \frac{\chi}{2}\frac{\partial^2 Y_c}{\partial Z^2} + \dot{\omega}_c^{HR}(Z, Y_c) \tag{3}$$

In eq. (3), Y_c is the progress variable, defined as a mass species fractions linear combination, which describes the chemical evolution. Consequently, the ADF model establishes two hypotheses, namely, to solve only the flamelet equation for the progress variable and to decouple the chemical source term of the diffusion processes. Although,

at first glance, it may seem very restrictive constrains this model has been successfully applied to diesel-like sprays [6], diesel engines and furnaces [5, 14, 15]. For this work, the progress variable is defined as $Y_c = Y_{\mathrm{CO}} + Y_{\mathrm{CO_2}}$ [4]. Once the flamelet solutions are available, that depend on (Z, Y_c, a) for both DF and ADF models, the TCI is accounted for by means of presumed probability density functions (PDFs). In order to obtain the turbulent flame manifold, a beta PDF is used for mixture fraction fluctuations while a log-normal PDF is used for the variability in the scalar dissipation rate direction [1]. No fluctuations are accounted for the progress variable dimension. This TCI description leads to

$$\widetilde{\psi}(\tau, \widetilde{Z}, S, \overline{\chi_{st}}, \sigma) = \int_0^{\infty} \int_0^{Z_{sat}} \psi(\tau, Z, \chi_{st}) P_Z(Z, \widetilde{Z}, S) P_{\chi_{st}}(\chi_{st}, \overline{\chi_{st}}, \sigma)\, \mathrm{d}Z\, \mathrm{d}\chi_{st} \tag{4}$$

where ψ represents any variable and τ corresponds to the flamelet time. Mixture fraction PDF is defined by the mean mixture fraction, $\widetilde{Z}$, and its variance, $\widetilde{Z''^2}$, parametrized with the segregation factor S determined by $S = \widetilde{Z''^2}/((Z_{sat} - \widetilde{Z})\widetilde{Z})$. The variance of $\ln(\chi)$, σ^2, is assumed to be constant and equal to 2 [16].
The same procedure is applied to the scalar dissipation rate profile which gives $\widetilde{\chi}$. The ratio $\widetilde{\chi}$ and $\widetilde{Z''^2}$ is usually related to the inverse of a turbulent mixing time by a constant (C_χ) which leads to

$$\widetilde{\chi} = C_\chi \frac{\varepsilon}{k} \widetilde{Z''^2} \tag{5}$$

where k and ε are the turbulent kinetic energy and the rate of dissipation of turbulent kinetic energy, respectively.
In the CFD calculation, transport equations for $\widetilde{Z}$, $\widetilde{Z''^2}$ and for species mass fractions are solved together with the continuity, Navier-Stokes and enthalpy equations. The species chemical source terms are retrieved from the turbulent flame manifold, obtained from the integration by means of presumed PDFs of the flamelet database, following the formula:

$$\dot{\omega}_k = \frac{\widetilde{Y_k}^{tab}(\widetilde{Z}, S, \overline{\chi_{st}}, \widetilde{Y}_c(t + \delta\tau)) - \widetilde{Y_k}(t)}{\delta\tau} \tag{6}$$

where $\widetilde{Z}$, S, $\overline{\chi_{st}}$ and $\widetilde{Y_k}(t)$ are values related to the CFD cell and $\widetilde{Y_k}^{tab}$ is tabulated in the turbulent flame manifold. $\delta\tau$ is the time step for advancing in this manifold. The value $\widetilde{Y}_c(t + \delta\tau)$ is obtained from

$$\widetilde{Y}_c(t + \delta\tau) = \widetilde{Y}_c(t) + \frac{\partial \widetilde{Y}_c}{\partial t}(\widetilde{Z}, S, \overline{\chi_{st}}, \widetilde{Y}_c(t))\, \delta\tau \tag{7}$$

For this work, the flamelet manifolds have been solved with around 160 points in the mixture fraction direction (it depends on the Z_{sat} value) and a mesh of 504 points has been imposed for the progress variable with the aim of reducing uncertainties. For the turbulent combustion manifold around 32 values for $\widetilde{Z}$ have been kept, 17 for S ranging between 0 and 0.3 and around 35 values in the $\overline{\chi_{st}}$ direction are retained. The mesh imposed for the progress variable direction has 51 values following a parabolic distribution. The CFD time step is fixed at 10^{-7} s, which is considered enough small for describing the auto-ignition process and then, $\delta\tau$ is chosen equal to the CFD time step.
Finally, this work pretends to shed light on the influence of the chemical mechanism in turbulent spray simulations. For this purpose, three well-known mechanisms for the n-dodecane fuel, which is a diesel surrogate, available in the literature, have been used to carry out this study. The largest of them is the Narayanaswamy et al. with 255 species and 2289 reactions [17]. The Yao et al. mechanism, which has been specially addressed to the spray A, is an skeletal mechanism that consists of 54 species and 269 reactions [18]. Finally, the Wang et al. mechanism with 100 species and 432 reactions is the third and last mechanism that has been analyzed in the present work [19].

Parametric study

Experimental results correspond with those measured in the CPF facility available at CMT - Motores Térmicos [7, 8]. Two representative parametric sweeps have been chosen to accomplish this work. Boundary conditions are varied around the nominal conditions that is defined by an ambient temperature of $T_{amb} = 900$ K, an oxygen concentration of $X_{\mathrm{O_2}} = 0.15$ and a density of $\rho = 22.8$ kg/m^3. The first sweep is a parametric temperature variation with $X_{\mathrm{O_2}}$ = 0.15 and $\rho = 22.8$ kg/m^3. The second one varies in the oxygen concentration direction while keeping the ambient temperature at $T_{amb} = 900$ K and the density at $\rho = 22.8$ kg/m^3. The injection pressure is 150 MPa and the fuel temperature is 363 K for all the cases. The parametric cases description is gathered in table 1.
The injector has a nominal diameter of 90 μm, with nozzle reference 210675 [2]. The injection rate lasts for more than 4 ms in order to describe the quasi-steady fields. More details about the injection rate can be found in [6, 20].

Table 1. Definition of the spray A parametric studies.

X_{O_2}	T_{amb} (K)	ρ_{amb} (kg/m^3)	p_{amb} (MPa)	p_{inj} (MPa)	Z_{st}	Z_{sat}
0.13	900	22.8	5.98	150	0.040	0.326
0.15	750	22.8	4.97	150	0.046	0.251
0.15	800	22.8	5.3	150	0.046	0.278
0.15	850	22.8	5.63	150	0.046	0.303
0.15	900	22.8	5.96	150	0.046	0.326
0.21	900	22.8	5.91	150	0.063	0.325

Results and discussion

The set-up of the model is adjusted from the experimental inert spray A solution. For the sake of brevity this comparison is here omitted and the interested reader is referred to [6] whose set-up configuration has been directly taken for the present work.

Given that a flamelet model is used which in turn is based on the HRs solutions, the reactive comparison starts by the analysis of the ignition delay for the different chemical mechanisms provided by the HRs and the flamelet solutions. In this way, the behavior of the mechanisms is analyzed at different levels of complexity and the discrepancies between them can be tracked from the very beginning of the process until the final stage, that is, the turbulent spray. Figure 1 shows the ignition delay for the HRs and the flamelet with strain rate a =100 1/s, belonging to the representative strain rates of the flamelets related to the high temperature region of the turbulent flow [21], for the nominal case. The ignition delay is defined as the time of maximum rate of rise of the temperature for each mixture fraction, adopting a similar definition to that suggested by the ECN [2].

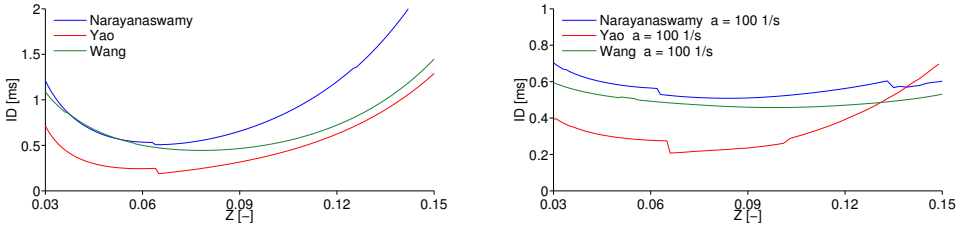

Figure 1. Ignition delay curves as a function of the mixture fraction for the HRs (left) and the flamelet with strain rate a =100 1/s (right) ignition for the nominal case.

As it can be deduced from figure 1, the Narayanaswamy and Wang mechanisms provide similar ignition delay profiles, in lean and slightly rich mixtures for the case of the ignition of the HRs and in the whole range of mixture fraction for the case of the flamelet, while the Yao mechanism exhibits the fastest ignition, with a minimum value around 200 μs, as it has been reported in the frame of the ECN [25].

The previous comparison is followed by the global parameters of the turbulent reactive spray, namely, the ignition delay and lift-off length. The ECN ignition delay criterion, namely, the time spent from start of injection (SOI) until the maximum rise of maximum Favre-averaged temperature takes place [2], is here applied. Although different definitions can be found for the LOL in the literature [2, 22], in this work, the criterion based on the minimum axial distance to the nozzle where 14 % of the maximum value of $\widetilde{Y_{OH}}$ in the domain is reached is adopted, given the satisfactory results that provides [6]. Figures 2 and 3 show the ID and LOL results for both parametric studies for the different chemical mechanisms. Additionally, experimental results are included with the nominal value and the uncertainty, given by error bars. In the temperature parametric variation none of the LOL values stabilized during the injection time (>4 ms) for the 750 K case and, hence, no value has been assigned.

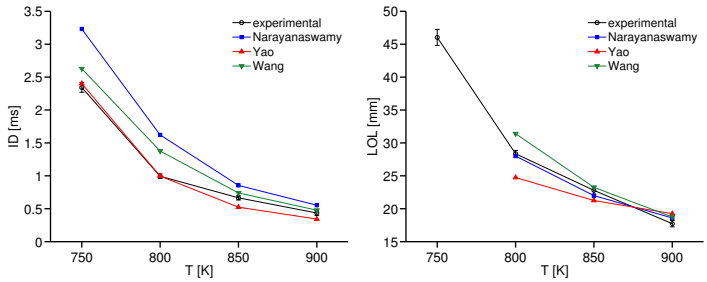

Figure 2. ID (left) and LOL (right) parameters for the temperature parametric variation (X_{O_2} = 0.15, ρ = 22.8 kg/m^3).

Attending to figure 2 it is clear that the Yao mechanism provides excellent results for ID even though, as it was mentioned before, it is addressed for spray A calculations [18]. Both Narayanaswamy and Wang mechanisms

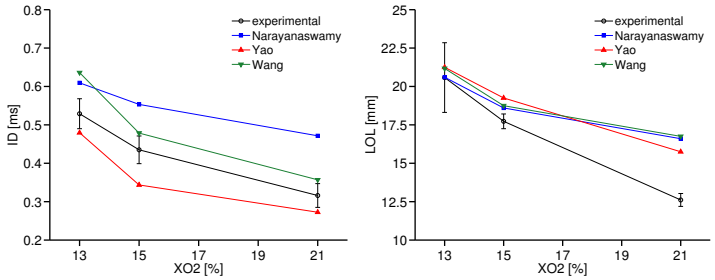

Figure 3. ID (left) and LOL (right) parameters for the oxygen parametric variation (T_{amb} = 900 K, ρ = 22.8 kg/m^3).

overestimate the ID and the values provided by the Narayanaswamy are greater than those corresponding to the Wang mechanism [23]. Nevertheless, the experimental trends are correctly reproduced. In terms of LOL, the Narayanaswamy mechanism is the one which better fits the LOL although the others give reasonable results.
With regard to oxygen sweep the Yao and Wang mechanisms follow a similar trend for the ID although the first one underestimates it while the second one overestimates it. The Narayanaswamy overestimates ID measurements [23] and is the mechanism which shows less sensitivity with the oxygen variation. For the LOL parameter, all three mechanisms provide very close values between them that are far from the experimental result for $X_{O_2} = 0.21$ and show low sensitivity when changing the oxygen concentration compared to the experiment.
In conclusion, in qualitative terms, the three mechanisms show acceptable trends for ID and LOL. In quantitative terms, the Yao mechanism seems that is the one that best fits the ID, especially for the temperature parametric variation [18]. As it is observed, in general, the Yao mechanism shows the fastest ignition followed by the Wang mechanism and, finally, by the Narayanaswamy mechanism, in line with the trends given by the ignition for the HRs and the flamelet shown in figure 1 for the nominal case.
Finally, it is important to note that the previous results show that when the ID is decreased the LOL is reduced too [26], pointing out to the auto-ignition phenomenon as an stabilization flame mechanism and, hence, to the relevance of the chemical kinetics involved in the combustion process for diesel engine conditions [1].
Apart from the global parameters trends, a deeper insight is provided by analyzing the temperature and species spatial fields for the different chemical mechanisms. For that purpose, figure 4 shows the solutions for the nominal case for the temperature and three representative species, namely, formaldehyde (CH_2O), a tracer of the low and intermediate temperature reactions, hydroxide (OH), a tracer of the high temperature reactions and, finally, acetylene (C_2H_2), a soot precursor. The experimental and modeled LOL values are included together with the stoichiometric level curve. The fields correspond to very advanced time instants (3000 μs) when a considerable section of the spray has reached quasi-steady regime.

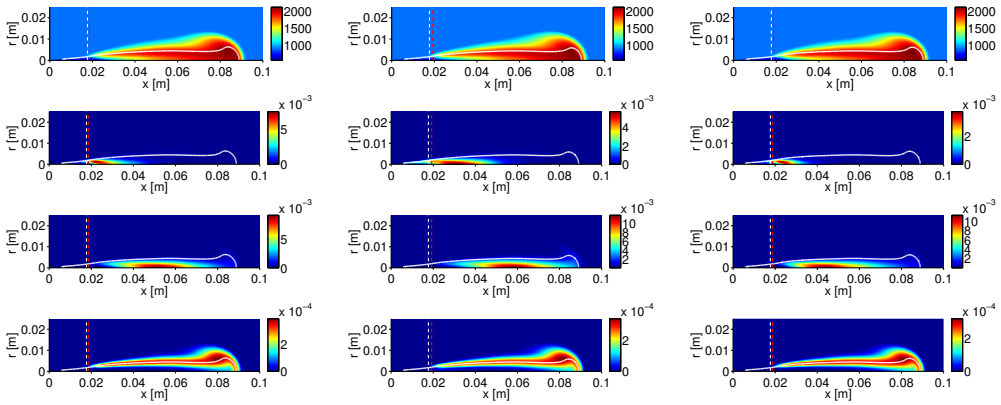

Figure 4. Temperature (top) and species mass fractions fields of CH_2O (middle top), C_2H_2 (middle bottom) and OH (bottom) for the nominal case (T_{amb} = 900 K, X_{O_2} = 0.15 and ρ = 22.8 kg/m^3) for the Narayanaswamy (left), Yao (center) and Wang (right) chemical mechanisms. LOL values are included with dashed lines: experimental (white) and 14% $\widetilde{Y_{OH}}^{max}$ (red). Additionally, the stoichiometric line is shown (solid white).

Attending to the results gathered in figure 4, it is clear how the three mechanisms provide similar results for the high temperature regions and, consequently, the spatial fields and the maximum values for the temperature and OH fields do not show noticeable discrepancies. Nevertheless, the low temperature regions are the zones where differences are more stringent as can be deduced from the CH_2O field and, in a less accused way, from the C_2H_2 field. The CH_2O field considerably changes among mechanisms as well as its maximum value reached in the domain.
In general, the fields provided by the Narayanaswamy and the Wang mechanisms are similar [23] and the Yao mech-

anism is the one that shows greater differences, especially for the CH_2O that extends in a wider region compared to the other mechanisms.
A clearer description of the combustion process is evidenced when the species are represented in the equivalence ratio-temperature or ϕ-T maps. Species CH_2O, C_2H_2 and OH are drawn, only including the points of the domain that verify the condition $Y_i > 0.3 \cdot Y_i^{max}$ where i represents the species CH_2O, C_2H_2 or OH and the superscript max refers to maximum value in the domain. Additionally, the curve of maximum temperature as a function of ϕ during the combustion onset is included. Figures 5 and 6 show these ϕ-T maps for the parametric variation in temperature and oxygen concentration. Results correspond to very advanced instants (>3500 μs).

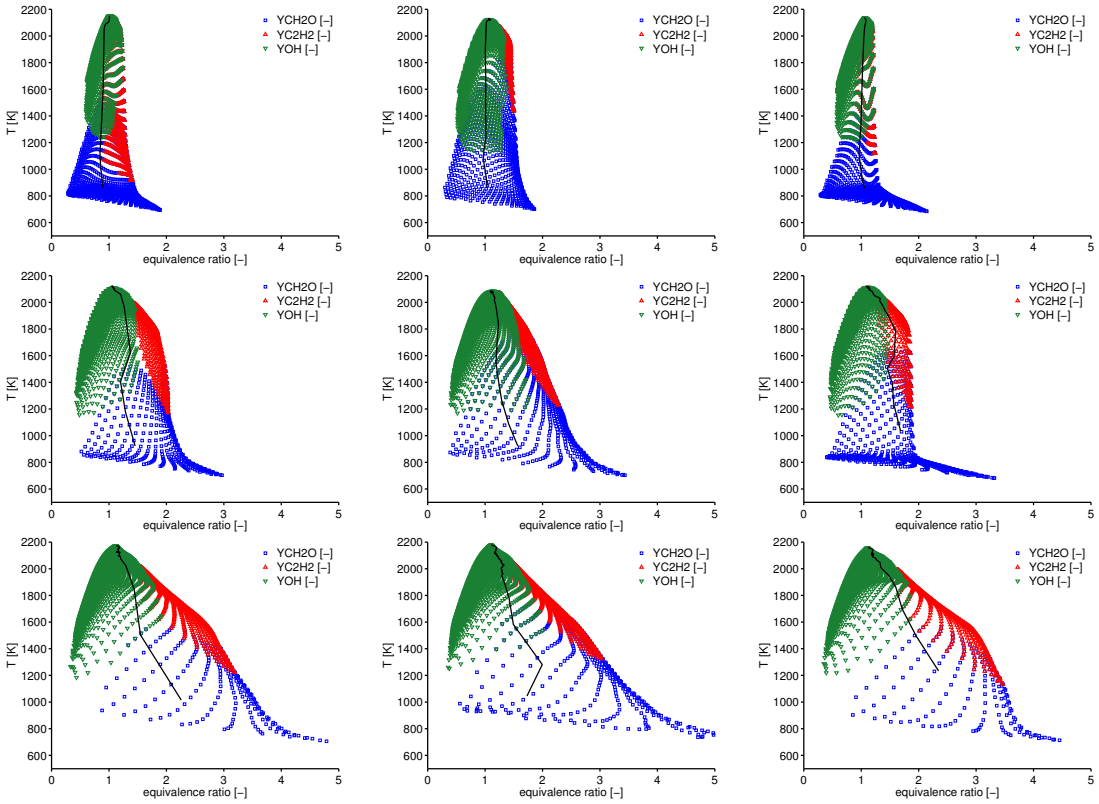

Figure 5. ϕ-T maps for the temperature parametric variation ($X_{O_2} = 0.15$, $\rho = 22.8$ kg/m^3) for 750 K (top), 800 K (middle) and 900 K (bottom) for the Narayanaswamy (left), Yao (center) and Wang (right) chemical mechanisms. The onset of the combustion in terms of maximum temperature as a function of ϕ is included in solid black line. Scales are common for all cases.

Figures 5 and 6 show that the low and intermediate temperatures and rich mixtures (CH_2O and C_2H_2) are the zones more affected by the selection of the chemical mechanism while the high temperature region (OH) is very similar for all the mechanisms, as was pointed out in figure 4. Consequently, the formaldehyde is especially affected by the chemistry as well as the contour of the map, which delimits the region of reactive mixtures, that is clearly different for rich mixtures between mechanisms. The zone where the reactive mixtures extend in the ϕ-T map is important because it determines the prediction of pollutant emissions by the model [24]. It is observed that the Wang mechanism shows the most accused slopes in the contour of the map for rich mixtures and, on the contrary, the softest slopes at these mixtures correspond to the Yao mechanism.
The differences between chemical mechanisms are accentuated when decreasing (by the boundary conditions) the reactivity of the mixture either by the reduction of the ambient temperature or the oxygen concentration.
With regard to the high temperature combustion onset, represented by the transient evolution of the maximum temperature as a function of the equivalence ratio, the Wang mechanism shows that the ignition kernels appear at ϕ>2 or even richer, the Narayanaswamy provides a similar evolution although at leaner mixtures while, following the Yao mechanism, this onset occurs at slightly rich mixtures. The maximum temperature reached in the domain does not depend on the chemical kinetics.
In terms of species, the Narayanaswamy and Wang mechanisms show similar behavior while the Yao mechanism is the one that exhibits more stringent discrepancies denoted by the wide region where formaldehyde appears and the greater reactivity of the rich mixture fractions.
In conclusion, it is deduced that the low temperature region, where the LOL establishes and close to the region where soot is nucleated, is the most affected zone by the chemical mechanism while no relevant differences arise for the high temperature chemistry.

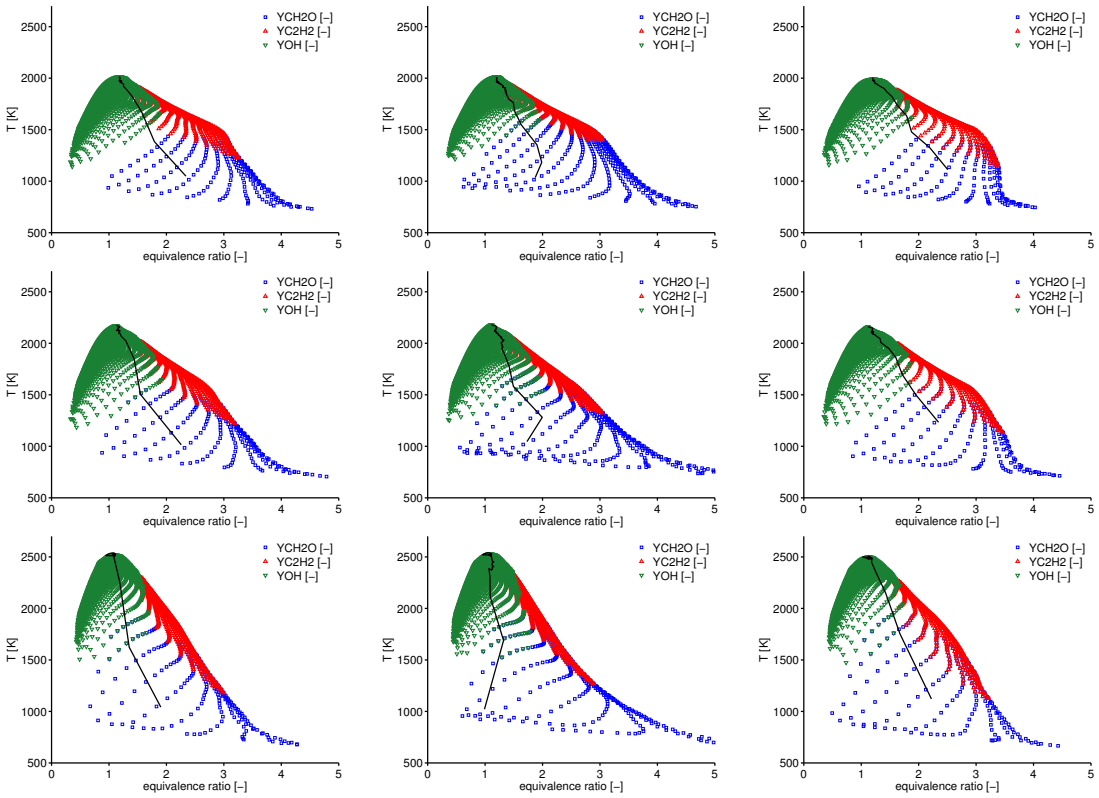

Figure 6. ϕ-T maps for the oxygen parametric variation (T_{amb} = 900 K, ρ = 22.8 kg/m^3) for X_{O_2} =0.13 (top), 0.15 (middle) and 0.21 (bottom) for the Narayanaswamy (left), Yao (center) and Wang (right) chemical mechanisms. The onset of the combustion in terms of maximum temperature as a function of ϕ is included in solid black line. Scales are common for all cases.

Finally, to end up this comparison, the temporal evolution of the total mass fraction of some relevant species appearing in the combustion (CH_2O, C_2H_2, CO, CO_2 and H_2O) are included in figures 7 for the nominal case.
It is observed in figure 7 that the three mechanisms give an excellent agreement for the temporal evolution of the masses related to final species, such as CO_2 and H_2O and intermediate species such as CO. Nevertheless, intermediate species that appear in the region of rich mixtures and intermediate/high temperatures, such as CH_2O and C_2H_2, show important discrepancies between mechanisms. Hence, it is concluded that the selection of the chemical scheme is relevant for describing the structure of the combustion as well as for predicting soot formation but not for the calculation of thermochemical parameters related to the high temperature chemistry and/or equilibrium flame conditions.
As a final remark, figure 7 evidences that the C_2H_2, a soot precursor, is notably greater for the Yao mechanism with regard to the other schemes and, hence, it is expected that the Yao mechanism predicts greater soot formation.

Conclusions

One of the major concerns when simulating combustion devices is related to the description of the chemistry provided by the chemical mechanism. Hence, it is considered of scientific interest to give some insight about the influence of the mechanism not only in homogeneous conditions but in the turbulent spray itself.
For that purpose, in this work, the spray A, which is representative of the modern diesel engine combustion, has been modeled by means of the presumed PDF ADF unsteady flamelet model. Three chemical mechanisms for the n-dodecane, widely extended in the scientific community, have been analyzed, namely, Narayanaswamy, Yao and Wang mechanisms.
The three schemes well reproduce the trends of the parametric sweeps in terms of global parameters (ID and LOL) although the Yao mechanism systematically provides faster ignition.
In general terms, the Narayanaswamy and Wang mechanisms show similar behavior while the Yao mechanism departs from the other two.
According to the ϕ-T maps it is observed that the region of high temperatures is hardly affected by the selection of the chemical mechanism but the zone of low and intermediate temperatures and rich mixtures, in the vicinity where the LOL is established and the soot is nucleated, is the region where the mechanism shows more clear influence.
Finally, the mass temporal evolution of relevant species appearing during the combustion confirms that the chemical kinetics scheme has a considerable impact for tracking the evolution of the intermediate species, particularly, for soot predictions, as well as for the combustion flame structure. Nevertheless, the selection of the mechanism has

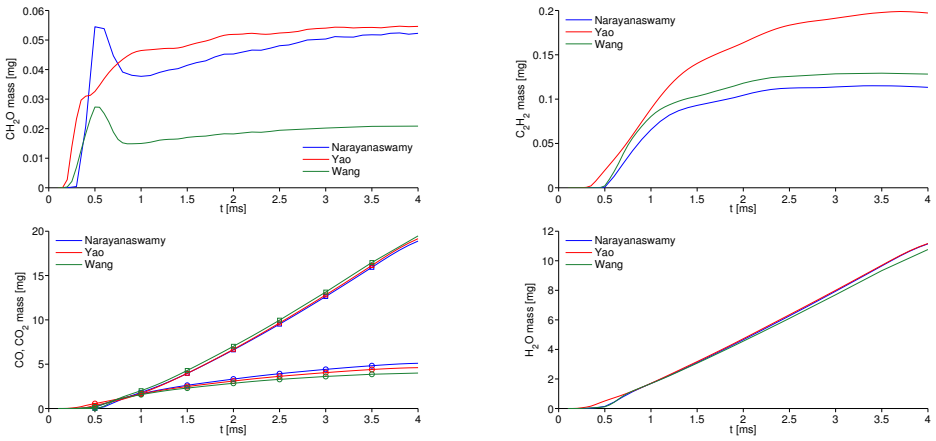

Figure 7. Mass temporal evolution of CH_2O (top left), C_2H_2 (top right), CO (circles) and CO_2 (squares) (bottom left) and H_2O (bottom right) species for the nominal case and the different mechanisms.

less influence for final species and thermochemical parameters related to the high temperature combustion.

Acknowledgements

Authors acknowledge that this work was possible thanks to the Ayuda para la Formación de Profesorado Universitario (FPU 14/03278) belonging to the Subprogramas de Formación y de Movilidad del Ministerio de Educación, Cultura y Deporte from Spain. Also this study was partially funded by the Ministerio de Economía y Competitividad from Spain in the frame of the COMEFF (TRA2014-59483-R) national project.

References

[1] Poinsot, T. and Veynante, D., 2005, "Theoretical and numerical combustion". RT Edwards Inc.
[2] Engine combustion network, https://ecn.sandia.gov/ ([cit. 2017-03-09]).
[3] Bardi, M., Payri, R., Malbec, L. M., Bruneaux, G., Pickett, L. M., Manin, J., Bazyn, T., Genzale, C. L., 2012, *Atomization and Sprays*, 22 (10).
[4] Michel, J. B., Colin, O., Veynante, D., 2008, *Combustion and Flame*, 152 (1), pp. 80-99.
[5] Tillou, J., Michel, J. B., Angelberger, C., Veynante, D., 2014, *Combustion and Flame*, 161 (2), pp. 525-540.
[6] Desantes, J. M., García-Oliver, J. M., Novella, R., Pérez-Sánchez, E. J., 2017, *Applied Thermal Engineering*, 117, pp. 50-64.
[7] Benajes, J., Payri, R., Bardi, M., Martí-Aldaraví, P., 2013, *Applied Thermal Engineering*, 58 (1), pp. 554-563.
[8] Payri, R., García-Oliver, J. M., Xuan, T., Bardi, M., 2015, *Applied Thermal Engineering*, 90, pp. 619-629.
[9] OpenFOAM http://www.openfoam.com/ ([cit. 2017-03-09]).
[10] Desantes, J. M., Garcia-Oliver, J. M., Pastor, J. M., Pandal, A., 2016, *Atomization and Sprays*, 26 (7).
[11] Pope, S. B., 1978, *AIAA journal*, 16 (3), pp.279-281.
[12] Barths, H., Hasse, C., Bikas, G., Peters, N., 2000, Proceedings of the Combustion Institute.
[13] Akkurt, B., Akargun, H. Y., Somers, L. M. T., Deen, N. G., Novella, R., Pérez-Sánchez, E. J., 2017, *SAE Technical Paper*
[14] Michel, J. B., Colin, O., 2013, *International Journal of Engine Research*, 15 (3), 346-369.
[15] Colin, O., Michel, J. B., 2016, *Flow, Turbulence and Combustion*, 97 (2), 631-662.
[16] Naud, B., Novella, R., Pastor, J. M., Winklinger, J. F., 2015, *Combustion and Flame*, 162 (4), pp. 893-906.
[17] Narayanaswamy, K., Pepiot, P., Pitsch, H., 2014, *Combustion and Flame*, 161 (4), pp. 866-884.
[18] Yao, T., Pei, Y., Zhong, B. J., Som, S., Lu, T., Luo, K. H., 2017, *Fuel*, 191, pp. 339-349.
[19] Wang, H., Ra, Y., Jia, M., Reitz, R. D., 2014, *Fuel*, 136, pp. 25-36.
[20] CMT - Motores Térmicos, Universitat Politècnica de València, Spain, http://www.cmt.upv.es/ECN03.aspx ([cit. 2017-03-09]).
[21] Bekdemir, C., Somers, L. M. T., de Goey, L. P. H., 2011, Proceedings of the Combustion Institute.
[22] Bajaj, C., Ameen, M., Abraham, J., 2013, *Combustion Science and Technology*, 185 (3), pp. 454-472.
[23] Frassoldati, A., D'Errico, G., Lucchini, T., Stagni, A., Cuoci, A., Faravelli, T., Onorati, A., Ranzi, E., 2015, *Combustion and Flame*, 162 (10), pp. 3991-4007
[24] Kamimoto, T., Bae, M., 1988, *SAE Technical Paper*.
[25] Hawkes, E., Sep. 6 2015, Fourth Workshop of the Engine Combustion Network, https://ecn.sandia.gov/ ([cit. 2017-03-09]).
[26] Pickett, L. M., Siebers, D. L., Idicheria, C. A., 2005, *SAE Technical Paper*.